ELSEVIER

Journal of Nuclear Materials 283–287 (2000) 508–512

journal of nuclear materials

www.elsevier.nl/locate/jnucmat

Effect of strain rate on the tensile properties of unirradiated and irradiated V–4Cr–4Ti

A.F. Rowcliffe *, S.J. Zinkle, D.T. Hoelzer

Oak Ridge National Laboratory, P.O. Box 2008, Bldg. 5500, Oak Ridge, TN 37831-6376, USA

Abstract

Tensile tests were carried out on an annealed, unirradiated V–4Cr–4Ti alloy from RT to 850°C at strain rates ranging from 10^{-1} to 10^{-5} s^{-1}. Below 300°C, where interstitial solutes are relatively immobile, deformation is homogeneous, and the strain rate sensitivity (SRS) of the yield and flow stress is positive. Between 300°C and 700°C, the formation of solute atmospheres at locked dislocations results in dynamic strain-aging (DSA), deformation becomes heterogeneous, and the SRS of the flow stress is negative; in this regime the lower yield stress is independent of strain rate. Above 700°C, substitutional solutes are also mobile, DSA declines, and the material enters a power law creep regime in which the SRS becomes positive again. Following neutron irradiation to 0.5 dpa at temperatures $\leqslant$400°C, severe flow localization occurs due to the high number density of $\langle 1\,1\,0\rangle$ and $\langle 1\,1\,1\rangle$ loops. However, above 400°C, strain hardening capacity returns but without the Lüders extension. At 500°C, after several percent plastic deformation, DSA occurs as interstitial solutes are released from the defect structure.

1. Introduction

A vanadium alloy containing 4 wt% Cr and 4 wt% Ti is currently being assessed by the US Fusion Materials Program as a potential structural material. The mechanical behavior of BCC alloys is strongly influenced by the behavior of the interstitial species C, O, and N, and the V–4Cr–4Ti alloy is no exception. In spite of the presence of 4 wt% Ti, which interacts strongly with the interstitials, the alloy exhibits the classic features of yield drop, Lüders extension, and dynamic strain aging during tensile testing. The present work was undertaken to explore the effects of temperature, strain rate, and low-dose irradiation on these phenomena, and to provide a basis for developing the constitutive laws that are necessary for an understanding of fracture behavior.

2. Experimental

Sheet tensile specimens of the SS-3 type (nominal gage dimensions $0.76 \times 1.52 \times 7.6$ mm^3) were prepared from 40% cold-rolled (CR) plate material from a 500 kg heat of V–4Cr–4Ti (Teledyne Wah-Chang heat no. 832665). After machining, specimens were annealed at 1000°C for 2 h in a vacuum of 10^{-6} Torr. The processing, which has been described in detail [1], resulted in a uniform microstructure with a grain size of $\sim$23 μm, a hardness of $\sim$ 137 DPH, and a room temperature resistivity value of 281.9 Ω m. The interstitial contents were, in weight ppm 79 C, 310 O, 85 N. Tensile testing was carried out using a screw driven machine at strain rates ranging from 10^{-1} to 10^{-5} s^{-1}, under a vacuum of $\sim 2 \times 10^{-7}$ Torr. SS-3 and TEM specimens were irradiated in the high flux beam reactor (HFBR) at Brookhaven to a neutron dose of 0.5 dpa at temperatures ranging from 160°C to 420°C and to a dose of 0.1 dpa at 505°C. Pre- and post-irradiation resistivity measurements showed that the interstitial content of the alloy did not increase during irradiation. Full details of these experiments may be found in [2]. Following irradiation, testing was carried out in a vacuum of $< 2 \times 10^{-6}$ Torr at the irradiation temperature with strain rates ranging from 10^{-2} to 10^{-5} s^{-1}.

* Corresponding author. Tel.: +1-423 574 5057; fax: +1-423 574 0641.

E-mail address: af8@ornl.gov (A.F. Rowcliffe).

0022-3115/00/$ - see front matter
PII: S0022-3115(00)00311-1

3. Results

3.1. Unirradiated tensile behavior

The tabulated data from testing at nine temperatures and five strain rates may be found in [3]. The main features of the tensile curves for V–4Cr–4Ti are illustrated in Fig. 1, which contains data from 20°C to 850°C obtained at a strain rate of 10^{-3} s^{-1}; for clarity, the original curves are offset from the stress and strain axes.

For most of the curves, the end of the elastic regime is followed by a small plastic pre-strain, followed by a Lüders extension that typically ranges from 0.5% to 1.0%. At 20°C, the Lüders extension is preceded by a prominent load drop, however, at higher temperatures and at all strain rates examined, an initial load drop is barely detectable. The stress required to propagate the Lüders extension is defined in this work as the lower yield stress σ_y. Following the Lüders extension, deformation occurs throughout the specimen; eventually, the strain-hardening rate decreases and the ultimate tensile stress, σ_u, is achieved at the point of plastic instability. For temperatures between 300°C and 750°C, and at sufficiently low strain rates, serrations occur in various regions of the flow curves (Fig. 1). These serrations are related to the diffusion of solute atoms and the locking of dislocations during the test, i.e., the phenomenon of dynamic strain aging (DSA).

3.2. Irradiated tensile behavior

Tensile data for specimens of V–4Cr–4Ti irradiated in the HFBR experiment to 0.5 dpa were reported previously, and a full tabulation of the tensile data, including the effects of strain rate may be found in [2,4,5]. Tensile curves for V–4Cr–4Ti irradiated and tested at five different temperatures using a strain rate of $\sim 10^{-3}$ s^{-1} are presented in Fig. 2. For temperatures of $\leqslant$325°C, radiation hardening results in an almost two-fold increase in yield stress. In contrast to the unirradiated behavior (Fig. 1), yielding is immediately followed by plastic instability and strain softening; there is no Lüders extension. At 420°C, where hardening is less severe, yielding is followed by an extensive strain-hardening regime, although, again, there is no Lüders extension and the flow curve contains only a few well-spaced serrations.

At 550°C, the radiation-induced increase in σ_y is only $\sim$50 MPa. As before, there is no Lüders extension. At a strain rate of $\sim 10^{-3}$ s^{-1}, the flow curve is fairly smooth, but serrations appear after the accumulation of 4–5%

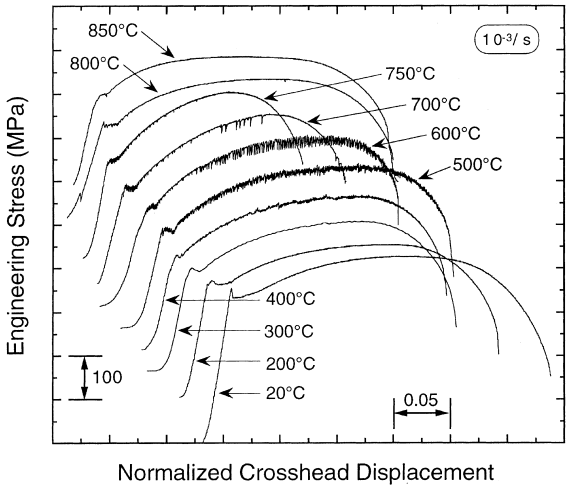

Fig. 1. Tensile curves for annealed V–4Cr–4Ti at a strain-rate of 10^{-3} s^{-1} illustrating DSA regime; curves offset on stress and strain axes for clarity.

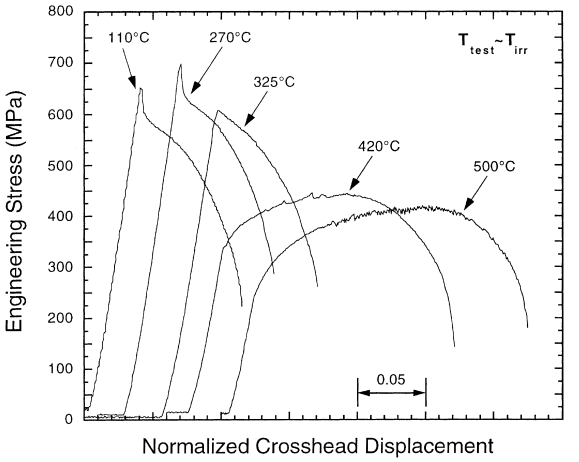

Fig. 2. Tensile curves for V–4Cr–4Ti irradiated in HFBR to 0.5 dpa at 110–420°C and to 0.1 dpa at 505°C; curves offset on strain axis for clarity.

Table 1
Strain rate sensitivity parameters

Test temperature (°C)	Lower yield stress (m)	Flow stress (m)	UTS (m)
Unirradiated			
20	0.025	0.019	0.017
300	0.077		
400	0.005	−0.014	−0.014
500	0.001	−0.017	−0.017
600	−0.002	−0.017	−0.028
700	−0.007	−0.021	−0.020
Irradiated			
160	0.008		0.008
200	0.010		0.010
400	0.005		0.016
500	0.010		−0.010

plastic strain. Lowering the strain rate increases the amplitude of oscillations.

The strain-rate sensitivity parameters (Table 1) were determined for tensile curves for V–4Cr–4Ti irradiated to doses ranging from 0.1 to 4.0 dpa and tested close to the irradiation temperature. The tensile data for 200°C and 400°C were reported in [4], and the data for 160°C and 500°C in [5].

4. Discussion

From the general relationship between flow stress and strain rate, the strain rate sensitivity (SRS) parameter is defined as follows [6]:

$$m = \frac{1}{\sigma}\frac{\delta\sigma}{\delta \ln \dot{\varepsilon}}\bigg|_{\varepsilon,T}. \quad (1)$$

Because slip is a thermally activated process, the flow strength increases with increasing strain rate, i.e., m is generally positive. However, in the DSA regime, increasing the strain rate decreases the time available for solute diffusion to dislocations, thus weakening the obstacle and lowering the flow strength, i.e. the SRS becomes negative. At low temperatures, solute mobility is too low for sufficient solute concentrations to be achieved and at high temperatures, solute atmospheres are too mobile to exert any significant drag. Thus, the DSA regime is bounded by certain values of temperature and strain rate and is characterized by negative values of the SRS parameters.

The lower yield stress, σ_y, and the flow stress, σ_f (defined here as the stress required to produce a plastic strain of 8%), were determined for each temperature and strain rate ($\dot{\varepsilon}$). These parameters are plotted against $\log \dot{\varepsilon}$ in Figs. 3 and 4. Values of the SRS parameters m were determined from a logarithmic fit to the data of Figs. 3 and 4; these values are summarized in Table 1.

Early work by Bradford and Carlson [7] on strain-aging effects in vanadium with oxygen contents ranging from 50 to 1800 wppm (subsequently reviewed by Baird [8]) predicts the occurrence of DSA at ~300°C for a strain rate of 10^{-4} s^{-1}. Edington et al. [9] observed DSA in vanadium containing 3000 wppm oxygen and tensile tested at 300–350°C at a strain rate of $\sim 10^{-4}$ s^{-1}. Thus, the present observations of DSA effects appearing at strain rates of $<10^{-3}$ s^{-1} at 300°C in the V–4Cr–4Ti alloy are consistent with the earlier work on pure vanadium. The internal friction measurements of Shikama et al. [10] provide evidence for a strong positive interaction between O, C, and the substitutional Ti atoms in V–Ti alloys. Further experimental evidence for a reduction in the mobility of interstitial solutes in the presence of Ti is provided by the results of Nakajima et al. [11], which indicate that the diffusivity of O in vanadium is decreased in a V–5% Ti alloy. Using the diffusivity data of Schmidt and Warner [12], the average diffusion distance ($\sqrt{Dt}$) for oxygen in pure vanadium at 300°C for the approximate time of a tensile at 10^{-4} s^{-1} is ~900 Å. From the data of Nakajima et al. $\sqrt{Dt}$ for the same conditions would be only ~1 Å in a V–5% Ti alloy. Thus, although these data indicate a strong binding between Ti and the interstitial solutes, it appears that a fraction of the interstitial solute population remains unbound and is sufficiently mobile to generate DSA phenomena in the V–4Cr–4Ti alloy.

For the lower yield stress, σ_y (Fig. 3), there appears to be three regimes of SRS that are related to the mobilities of various solute species. At low temperatures

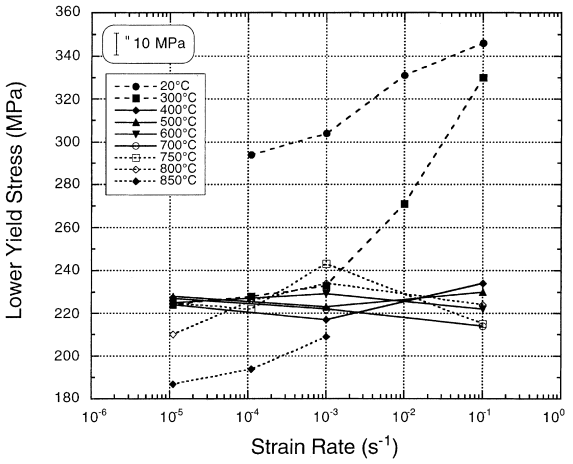

Fig. 3. Lower yield stress as a function of strain rate for various temperatures; SRS is positive at < 300°C. σ_y is strain-rate insensitive at 300–700°C; SRS becomes positive again at >700°C.

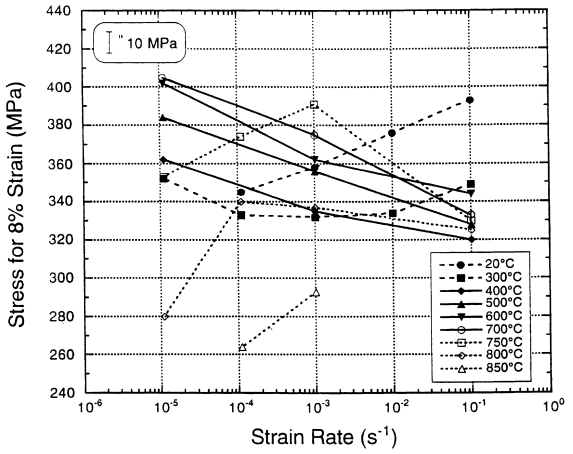

Fig. 4. Flow stress as a function of strain rate for various temperatures; SRS undergoes a transition from positive to negative at 300°C as DSA occurs. SRS becomes positive again above 700°C.

(<300°C), where the interstitial solutes are relatively immobile, the SRS of σ_y is positive, and ranges from 0.025 to 0.077. At intermediate temperatures (300–700°C) where the interstitials are mobile, the SRS parameter decreases and eventually becomes slightly negative (−0.002 to −0.007). Above 700°C and at strain rates below 10^{-3} s^{-1}, the SRS of σ_y becomes positive again. At these temperatures, in addition to the interstitial solutes being highly mobile, the substitutional solutes are also mobile.

The flow stress, σ_f, also exhibits a region of positive SRS for temperatures below 300°C. At 300°C, where C and O are mobile, the strain-rate dependence of σ_f displays a classic U-shape (Fig. 4) going from positive at high strain rates to negative at low strain rates. The transition to a negative SRS coincides with the appearance of serrated yielding in the Lüders region and jerky flow in the strain-hardening regime. Over the range 400–700°C, the SRS of the flow stress is negative for all strain rates, and all flow curves are strongly serrated. Above 700°C, the magnitude and frequency of the serrations decline, and at 800°C, serrations are confined to the Lüders region (Fig. 1). At temperatures above 700°C, and for strain rates below $\sim 10^{-3}$ s^{-1}, the SRS becomes positive again. Examination of the stress–strain curves at 750°C, 800°C, and 850°C for strain rates $<10^{-3}$ s^{-1}, where the SRS is positive, indicate that two significant changes in deformation mode occur in this regime. Firstly, the frequency and amplitude of the serrations in the flow curves decrease rapidly and are non-existent at 850°C. Secondly, at 750°C, when the strain-rate is decreased below 10^{-3} s^{-1}, after a small amount of plastic strain, strain hardening ceases, the ultimate tensile strength is lowered, and the total elongation increases. These changes strongly suggest that a transition has occurred into a power law creep regime.

The flow stress and the lower yield stress for V–4Cr–4Ti determined at a strain rate of 10^{-3} s^{-1} are shown as a function of temperature in Fig. 5. Three approximate temperature regimes of deformation behavior are indicated. In the regime below 300°C, where interstitial solutes are relatively immobile, both σ_f and σ_y decrease continuously with increasing temperature and the flow curves are smooth, indicating homogeneous deformation. At intermediate temperatures, between 300°C and 750°C, the interstitial species are mobile and the flow stress, σ_f, increases with increasing temperature due to dynamic strain-aging. Above 750°C, where Ti and V are also mobile, both σ_f and σ_y drop sharply with temperature with the onset of the power law creep regime.

Irradiation to 0.5 dpa completely alters deformation behavior (Fig. 2). For irradiation temperatures $\leqslant$400°C, the yield strength is approximately doubled by the development of a high number density of small

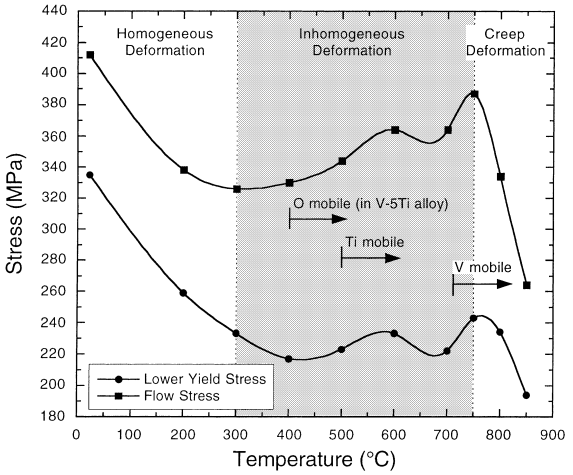

Fig. 5. Temperature dependence of σ_y and σ_f illustrating three deformation regimes.

(3–5 nm) loops [13]. Resistivity measurements indicate that a major fraction of the interstitial elements are associated with the loops [2]. High stresses are needed to unlock dislocation sources and because of dislocation channeling [13], failure occurs without any Lüders extension. Under these conditions, the lower yield stress, σ_y, coincides with the point of plastic instability. The SRS of σ_y for the irradiated materials is slightly positive over the entire range studied (160–500°C) in contrast to the unirradiated condition, where m is strongly positive below 300°C, decreases with increasing temperature, and becomes slightly negative above 500°C (Table 1).

At 425°C and 500°C, the population of $\langle 1\,1\,0\rangle$ and $\langle 1\,1\,1\rangle$ loops responsible for the low temperature hardening declines rapidly. The microstructure becomes dominated by fairly coarse $\{0\,0\,1\}$ defects, significantly enriched in Ti. These defects may be the precursors of the Ti $\{O\,C\,N\}$ precipitates observed at higher doses [14,15]. At 420°C, dislocation multiplication and strain hardening occur after yielding, but without a Lüders extension. The flow curve is fairly smooth except for a few well-spaced serrations. This behavior strongly suggests that the interstitial solutes are still trapped within the defect structure.

However, for the material irradiated and tested at $\sim$500°C, the flow curve is initially smooth but serrations appear after the accumulations of 4–5% plastic strain. The reason for this behavior is not known, although it is possible that since the free interstitial solute concentration is low, it is necessary to build up a sufficiently high dislocation density to reduce diffusion distances and allow significant solute concentrations to reach and pin dislocations.

5. Conclusions

1. Based upon tensile tests conducted at strain rates ranging from 10^{-1} to 10^{-5} s^{-1}, three different regimes of deformation behavior may be defined:
   (a) Below 300°C, where C, O, and N are relatively immobile, deformation occurs homogeneously and the strain rate sensitivity of the yield stress and flow stress are positive.
   (b) Between 300°C and 700°C, dynamic strain aging occurs, deformation becomes heterogeneous, and the SRS of σ_y becomes negative; in this regime the lower yield stress is essentially independent of strain rate.
   (c) Above 700°C, where substitutional solutes become mobile, DSA declines and the material enters a creep regime in which the SRS becomes positive again.
2. Although a strong interaction between Ti and interstitial impurities is indicated by diffusion data, a significant fraction of interstitials in this alloy are able to migrate freely and generate DSA phenomena in a temperature-strain rate regime similar to that for pure vanadium.

Acknowledgements

The authors acknowledge the efforts of C.O. Stevens in carrying out the tensile tests with care and attention to detail. This research was sponsored by the Office of Fusion Energy Sciences, US Department of Energy under contract DE-AC05-96OR22464 with Lockheed Martin Energy Research Corporation.

References

[1] A.F. Rowcliffe, D.T. Hoelzer, Fusion materials semiannual progress report, DOE/ER-0313/25, April 1999, p. 42.
[2] L.L. Snead, S.J. Zinkle, D.J. Alexander, A.F. Rowcliffe, J.P. Robertson, W.S. Eatherly, Fusion materials semiannual progress report, DOE/ER-0313/23, March 1998, p. 81.
[3] A.F. Rowcliffe, D.T. Hoelzer, S.J. Zinkle, Fusion materials semiannual progress report, DOE/ER-0313/26, September 1999, p. 25.
[4] S.J. Zinkle, L.L. Snead, J.P. Robertson, A.F. Rowcliffe, Fusion materials semiannual progress report, DOE/ER-0313/23, March 1998, p. 77.
[5] S.J. Zinkle, L.L. Snead, A.F. Rowcliffe, D.J. Alexander, L.T. Gibson, Fusion materials semiannual progress report, DOE/ER-0313/24, June 1998, p. 33.
[6] P. Haasen, Physical Metallurgy, Cambridge University, New York, 1978, p. 26.
[7] S.A. Bradford, O.N. Carlson Trans. Meter. Soc. AIME V. 224 (1962) 738.
[8] J.D. Baird, Metall. Rev. 149 (1971) 1.
[9] J.W. Edington, T.C. Lindley, R.E. Smallman, Acta. Metall. (1964) 1025.
[10] T. Shikama, S. Ishino, Y. Mishima, J. Nucl. Mater. 68 (1977) 315.
[11] H. Nakajima, S. Nagata, H. Matsui, S. Yamaguchi, Philos. Mag. A 67 (3) (1993) 557.
[12] F.A. Schmidt, J.C. Warner, J. Less Common Met. 26 (1972) 325.
[13] P.M. Rice, S.J. Zinkle, J. Nucl. Mater. 258–263 (1998) 1414.
[14] H.M. Chung, B.L. Loomis, D.L. Smith, J. Nucl. Mater. 212–215 (1994) 804.
[15] M. Satou, K. Abe, H. Kayano, J. Nucl. Mater. 212–215 (1994) 794.